Kovove Mater. 48 2010 127–135
DOI: 10.4149/km_2010_2_127

Deformation behaviour of pure aluminium during multi-pass equal channel angular pressing through route #C

S. S. S. Kumar*, I. Balasundar, T. Raghu

Near Net Shape Group, Defence Metallurgical Research Laboratory, Kanchanbagh, Hyderabad-500058, India

Received 14 October 2009, received in revised form 8 December 2009, accepted 10 December 2009

Abstract

Deformation behaviour of commercial pure aluminium during multiple pass equal channel angular pressing (ECAP) through route #C has been evaluated using finite element analysis. The results obtained indicate that a parallelogram shaped uniform plastic strain distribution can be obtained in the work piece. The plastic strain variation along the top, middle and bottom of the work piece along its length suggests that during multiple pass ECAP following route #C, a uniform plastic strain can be obtained in the work piece after every two passes if one can neglect the front and back end of the work piece. The length of these ends that need to be removed in ECAP processed work piece was found to be equal to the ECAP channel width (w). Further, it has been established that during multi-pass ECAP through route #C, the corner gap subtended by the work piece is independent of its geometry, whereas the load--displacement curve is dependent on the work piece geometry.

K e y w o r d s: equal channel angular pressing, finite element analysis, multi-pass, route #C

1. Introduction

The thrust behind producing bulk ultra fine grained (UFG) and nanostructured materials for their excellent mechanical properties [1] has led to the development of severe plastic deformation (SPD) processes like equal channel angular extrusion (ECAE) [2], accumulative roll bonding (ARB) [3, 4], high pressure torsion (HPT) [5], multi axial forging (MAF) [6], etc. Among the various SPD processes, ECAP developed by Segal [2, 7] is a promising technique to impart large plastic strain in bulk materials through single or multiple steps without any concomitant change in the work piece cross-sectional area. ECAP process involves pressing of a well lubricated work piece through a die containing two channels with identical cross-sections that intersect at two predetermined angles known as the channel angle (ϕ) and corner angle (Ψ). Simple shear plastic deformation occurs at the intersection of two channels as shown in Fig. 1. The strain imposed on the work piece during ECAP depends on the channel angle (ϕ), outer corner angle (Ψ), friction (μ or m), back pressure (P), etc. [8–12]. During multi-pass ECAP, the deformation behaviour and strain imparted are also influenced by processing routes. Different processing routes that have

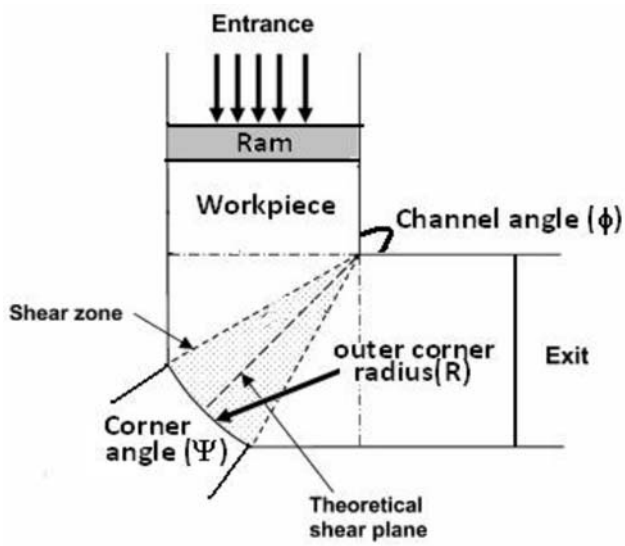

Fig. 1. Schematic of ECAP process.

*Corresponding author: tel.: +91 40 24586688; +91 9440191576; e-mail address: sssatheesh12@rediffmail.com

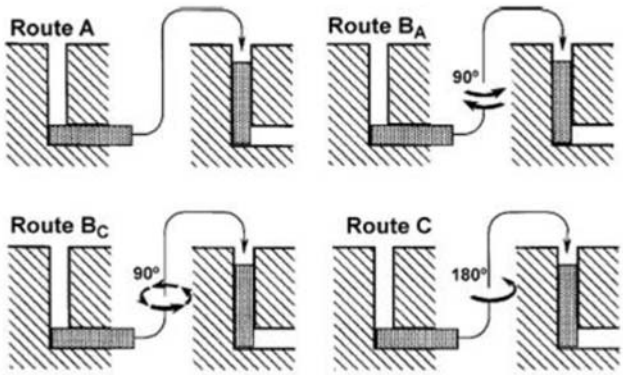

Fig. 2. ECAP processing routes.

been identified for multiple pass ECAP are shown in Fig. 2. It has been reported that a better strain uniformity can be achieved when a material is processed through either route B_c or C [13].

Finite element analysis (FEA) on ECAP so far has been extensively studied on single pass [14–17]; few multi-channel and multi-pass ECAP simulations have also been reported [18, 19]. In multi-channel ECAP, the work piece is pressed through continuous inter-connected channels in order to impart very large plastic strain without removing it from the die. Whereas in multi-pass ECAP, the work piece after every pass is removed from ECAP die and inserted back into the same or different die for subsequent processing. During multi-channel ECAP through inter-connected channels, the deformation behaviour and strain distribution behaviour are influenced by distance between the successive channels which is not the case in multi-pass ECAP. Though the effect of processing routes on the strain distribution has been analysed by various researchers [13, 20, 21], most of studies were extensively on route #B_c. Zhao et al. [22] have studied the deformation behaviour of pure aluminium through route #C. However, a detailed study on the strain distribution and the strain uniformity that can be achieved was not reported. In this work, the deformation behaviour and strain distribution in commercial pure aluminium subjected to multi-pass ECAP through route #C have been evaluated and reported.

2. Finite element analysis

The deformation behaviour of commercial pure aluminium at room temperature was simulated by car-

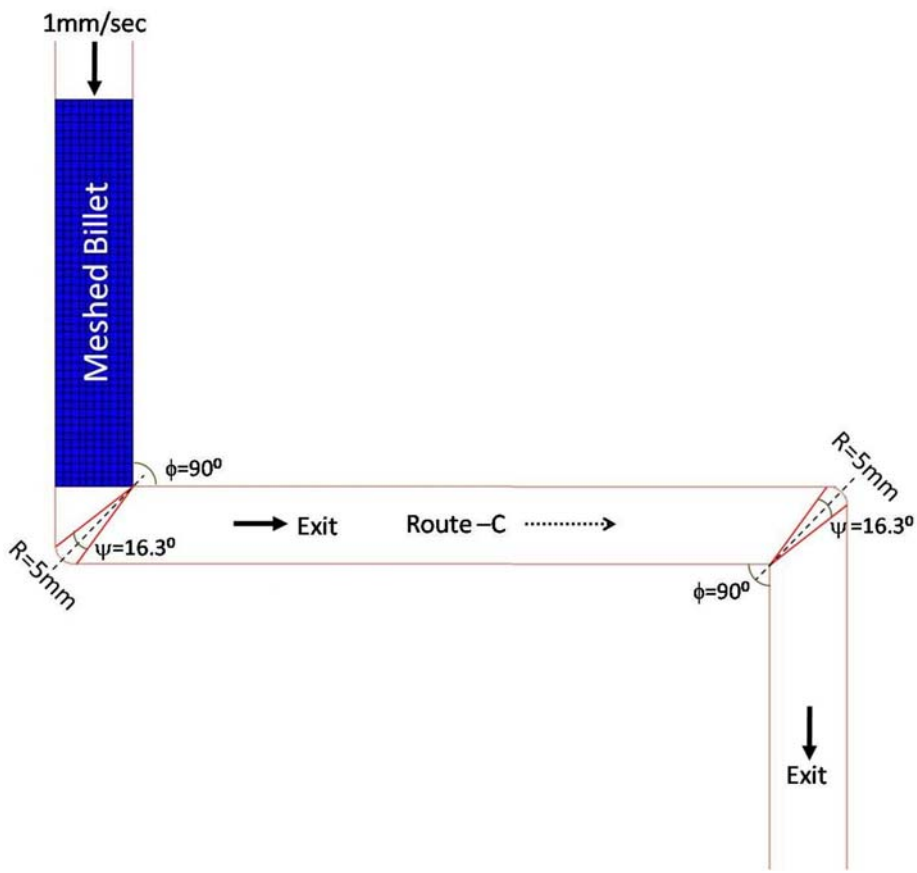

Fig. 3. ECAP die model used in FEM simulation.

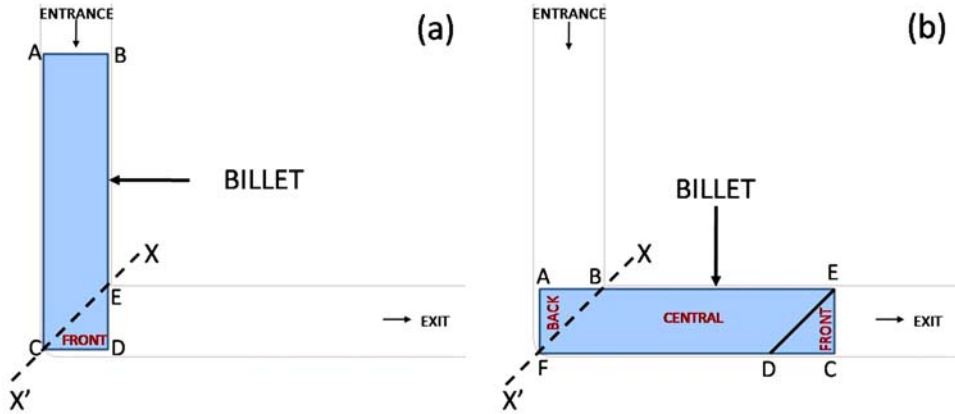

Fig. 4. Schematic of workpiece deformation during ECAP: (a) before ECAP, (b) after ECAP.

Table 1. Material properties of pure aluminium considered for simulation

Material properties	Value
Density, ρ	2.71 g cm^{-3}
Young's modulus, E	70 GPa
Poisson's ratio, ν	0.33
Strain hardening coefficient, n	0.304
Strength coefficient, K	173.79 MPa

rying out a plane strain two dimensional analysis using commercial finite element package MSc.Marc2007r1. ECAP die with a channel angle (ϕ) of 90° and corner angle (Ψ) of 16° 18′ which is equivalent to a fillet radii of 5 mm [10] shown in Fig. 3 was modelled as a non-deforming rigid body and was assumed to be stationary by imposing zero displacement boundary conditions. As it has been reported that the inhomogeneity of strain distribution increases with large corner angles [17, 23] and the strain distribution is not significantly altered up to a corner angle of ∼ 20° [24], a small corner angle (ψ) of 16° 18′ was selected for the present study. The work piece (20 × 20 × 100 mm^3) was assumed to be deformable with strain hardening characteristics (Table 1) and meshed with 4 node isoparametric quadrilateral elements. Though the initial mesh was coarse (500 elements), the number of elements were increased to 5000 before the start of the analysis and was held constant throughout the analysis. A suitable remeshing criterion was adopted to accommodate large strain during the deformation. The punch was assumed to be a non-deforming rigid body moving with a velocity of 1 mm s^{-1}. The punch velocity was controlled using a control file that contained the information on the number of step or sub steps to be taken. Route #C in ECAP corresponds to the rotation of work piece by 180° after every pass. The simulation of route #C was realized by reversing the entry and exit channel direction after every pass. All the finite element analyses were carried out under ideal frictionless conditions.

3. Results and discussions

3.1. Deformation pattern

During ECAP, the work piece experiences severe plastic deformation by simple shear at the region where the two channels intersect. This region is called as shear zone or plastic deformation zone (PDZ) as shown in Fig. 1. In order to evaluate the deformation behaviour during ECAP, the entire work piece length was divided into three zones, namely front, centre and back zone, as shown in Fig. 4. When the work piece is placed in the channel, the front end (CD) contacts the outer channel surface of die channel. It can be seen in Fig. 4a that an area CDE in work piece had already passed through the shear plane (XX') without undergoing any shear deformation even before the pressing had been initiated. Similarly at the end of ECAP process, an area ABF does not pass through the shear plane and is left undeformed as shown in Fig. 4b. The parallelogram shaped central zone marked by BEFD is the only region that experiences shear deformation. This sheared central zone is always inclined to the exit direction irrespective of the number of pass during multiple pass ECAP through route #C.

An asymmetric corner gap was observed when the work piece was pressed through the ECAP die with an outer corner angle of (ψ) 16° 18′ as shown in Fig. 5. The length of the gap was found to be more on the entry channel side than on the exit channel side as shown in Fig. 5a. It has been reported that the corner gap or corner angle made by the work piece is influenced by a number of factors such as friction [14, 10], back stress [9], deformation speed [25], strain hardening rate [10, 26]. Although a corner angle (ψ) of 16° 18′ was provided in the die, the corner gap or corner angle subtended by the work piece during ECAP was

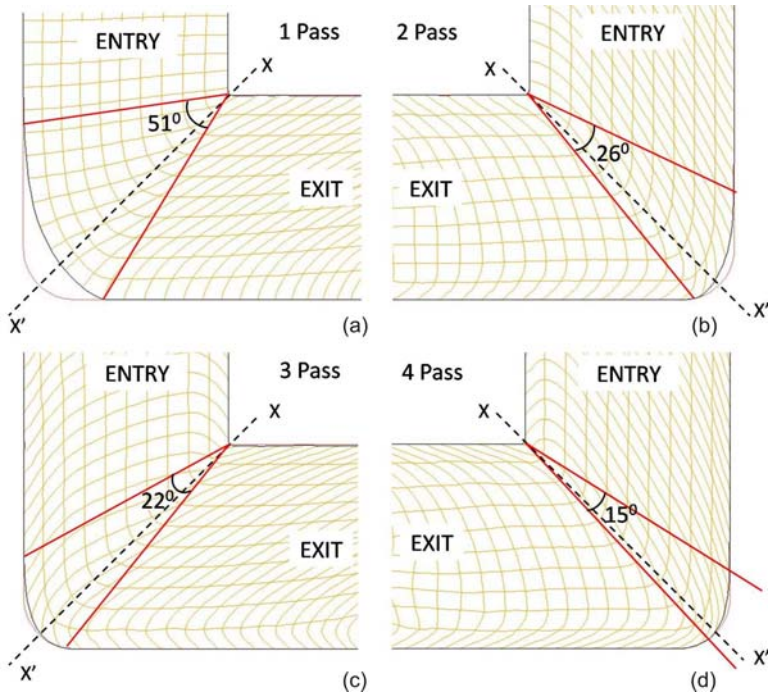

Fig. 5. Corner gap formation predicted by FEM.

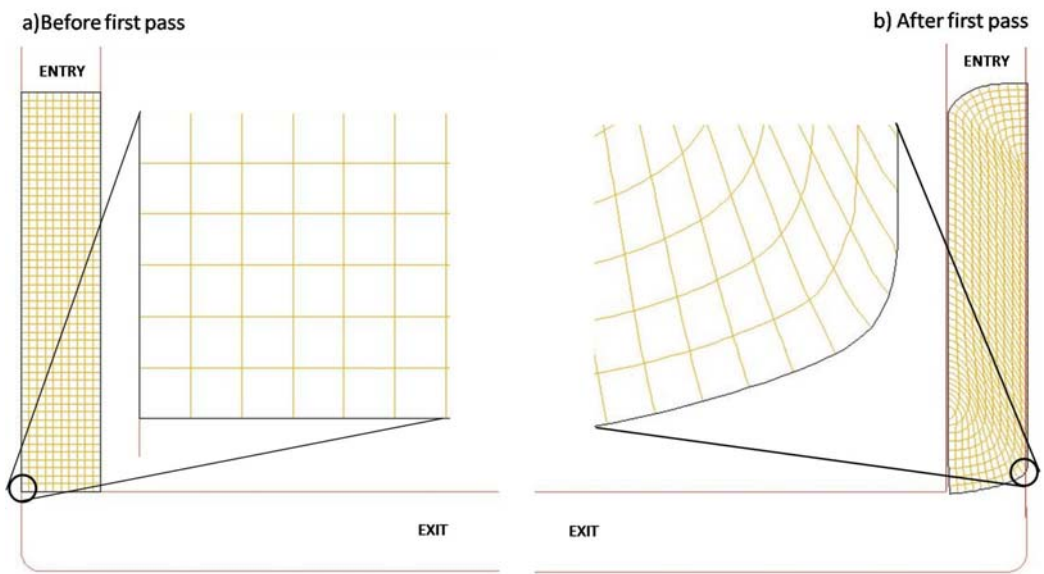

Fig. 6. Billet front end transformation.

found to be much higher. The corner angle formed by the work piece during ECAP through route #C after 1, 2, 3, and 4 passes was estimated to be 51°, 26°, 22°, and 15°, respectively. It was also observed that, as the number of ECAP passes increased, the gap at the exit channel side started decreasing and after 4 passes through route #C, no gap was observed on the exit side as shown in Fig. 5d. The decrease in corner angle during subsequent ECAP passes through route #C can be either due to the variation in work piece geometry or due to the variation in strain hardening rate of the material. During multi-pass ECAP through route #C, a change in the work piece geometry was observed after first ECAP pass. The flat front and back ends of work piece (Fig. 6a) were transformed into a round wedge shape ends after first pass as shown in Fig. 6b.

In order to study the effect of work piece shape on corner gap formation during ECAP, the transformed work piece geometry (round wedge shaped ends) after

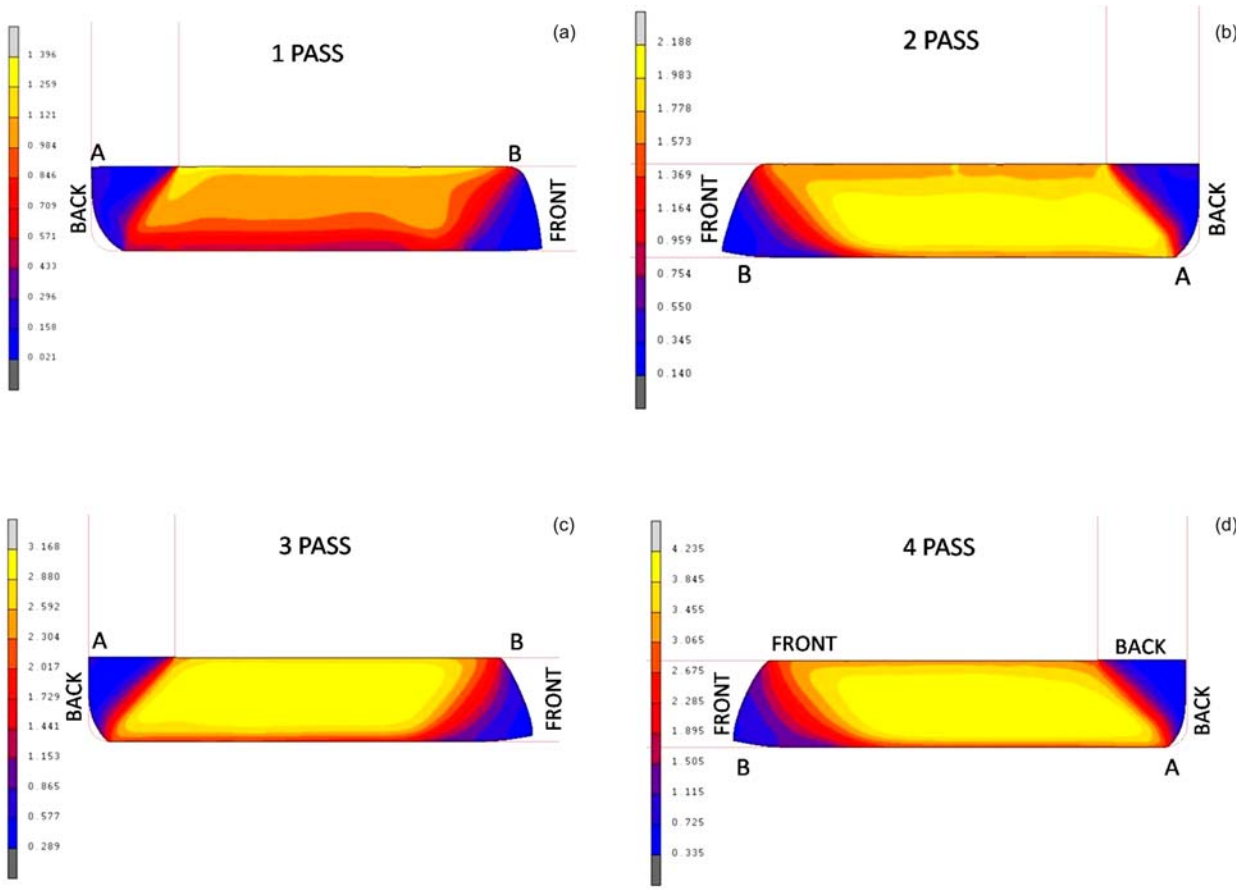

Fig. 7. FEM predicted plastic strain distribution across workpiece area after (a) 1st pass, (b) 2nd pass, (c) 3rd pass, (d) 4th pass.

first pass was considered as the initial work piece geometry and simulation was carried out following the procedure listed in Section #2. The corner gap formed by this work piece geometry was evaluated. Despite the presence of round cornered front end, a large corner gap was observed and the angle generated by the work piece was estimated to be 52°, which almost equals the corner angle formed by the regular work piece with flat ends. This clearly indicates that the corner gap formation during ECAP is independent of work piece geometry. Therefore, the decrease in the corner angle formed by the work piece during subsequent ECAP passes through route #C can be attributed to the decreasing strain hardening rate of the material.

3.2. Equivalent plastic strain distribution

The average equivalent plastic strain imparted during ECAP is influenced mainly by die channel angle (ϕ). A channel angle of 90° imparts an average equivalent plastic strain of 1.15 as per the analytical equation established by Iwahashi et al. [27]. The corner angle (ψ) has a marginal influence on the average equivalent plastic strain. In an ECAP die with a channel angle (ϕ) of 90°, the average equivalent plastic strain decreases from 1.15 to 0.907 when the corner angle changes from 0° to 90° [15]. The equivalent plastic strain distributions obtained through simulation after each ECAP pass through route #C are shown in Fig. 7. It can be seen that both the front and back end of work piece have experienced very less deformation, whereas the inclined central zone has been subjected to intensive shear deformation. The equivalent plastic strain distribution in the central zone after first pass was highly inhomogeneous, with higher plastic strain at the top surface relative to the bottom surface of the work piece. During the second ECAP pass via route #C (Fig. 7b), the work piece was rotated by 180°. As the work piece gets rotated by 180° along its length, the bottom surface of work piece becomes the top surface and vice versa for the second pass. After two ECAP passes, a parallelogram shaped uniform equivalent plastic strain region inclined along exit channel direction was obtained in the central zone of the work piece. However, the work piece ends had still experienced only very less deformation manifested by smaller equivalent plastic strains. At the end of the 3rd and 4th pass (Fig. 7c,d), although the inhomogeneity of strain distribution did not disappear,

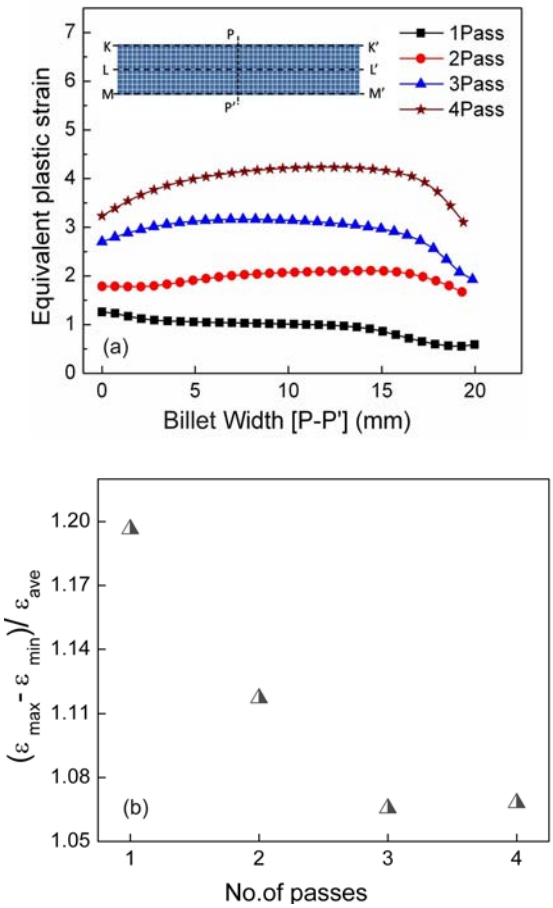

Fig. 8. (a) Plastic strain distribution across workpiece width and (b) variation of strain inhomogeneity.

the length of the uniform equivalent plastic strain region in the central zone had increased and was stable. The equivalent plastic strain experienced by the work piece was found to increase after every pass.

The equivalent plastic strain distribution across the work piece width from top to bottom in the central zone along P-P' after each ECAP pass through route #C was evaluated. It can be seen from Fig. 8a that after the first ECAP pass, the plastic strain is high at the top and decreases while traversing towards the bottom. However, after subsequent passes, due to the rotation of work piece after every pass, uniform strain distribution was observed in work piece centre, whereas low equivalent plastic strain was observed near the top and bottom surfaces. The strain inhomogeneity in the work piece after each ECAP pass through route #C was estimated using the expression reported by Suo et al. [28]. The strain inhomogeneity shown in Fig. 8b decreases initially during the first and second ECAP passes and thereafter remains fairly stable for the third and fourth ECAP pass.

The variation of equivalent plastic strain along the work piece length at the top (K-K'), middle (L-L'), bottom (M-M') were also evaluated and are shown in Fig. 9a–c. As one moves along the top surface of the work piece from the back or trailing end to front or leading end, it can be seen that the strain increases initially, remains constant for a certain length and thereafter decreases again. The length of this steady state region is ≈ 60 mm. A similar variation in the equivalent plastic strain was observed along the middle

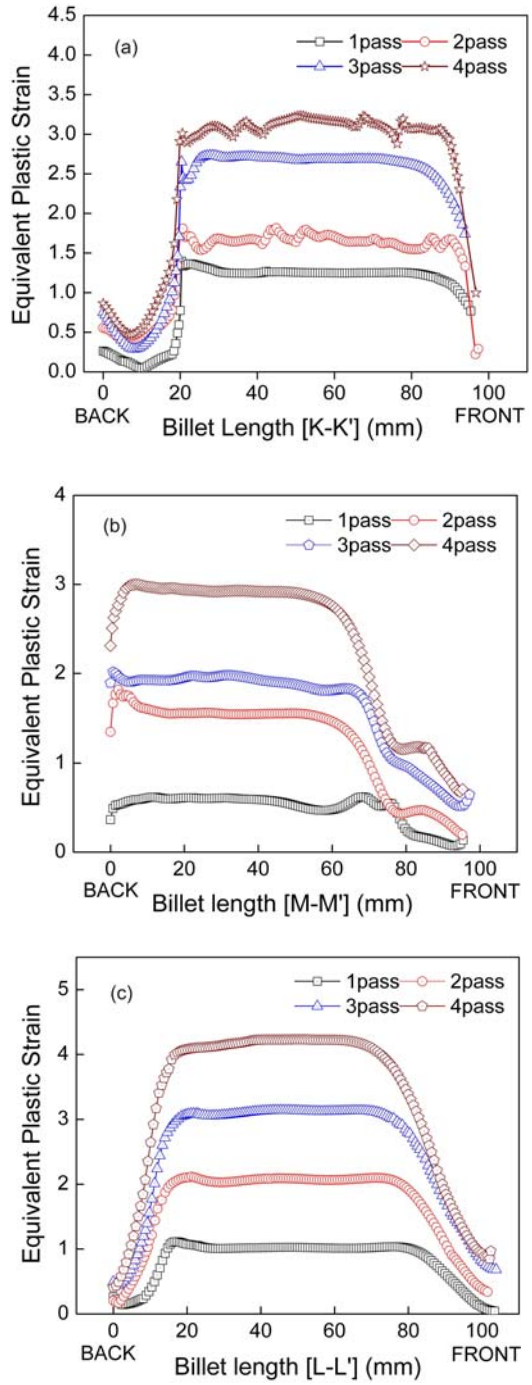

Fig. 9. Plastic strain distribution along workpiece: (a) top surface, (b) bottom surface, (c) mid surface.

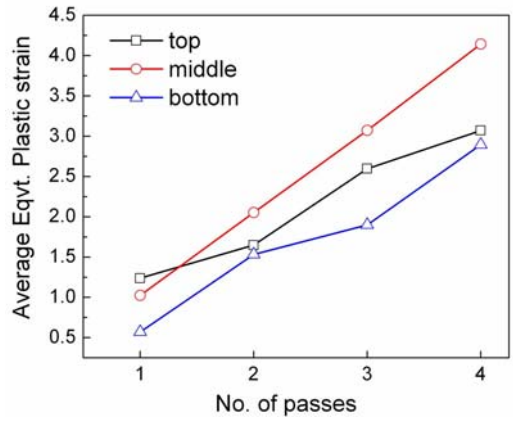

Fig. 10. Plastic strain variation across top, middle and bottom regions of billet.

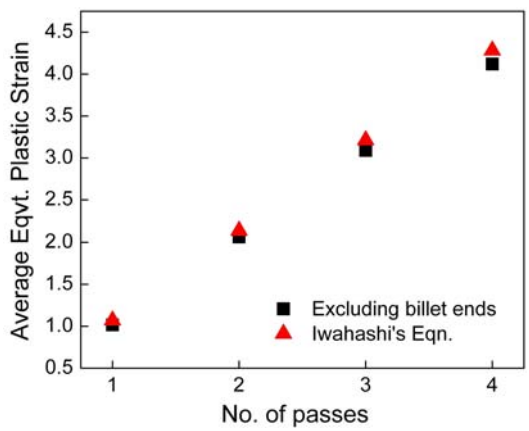

Fig. 11. Comparison of average equivalent plastic strain FEM simulation vs. Iwahashi's analytical equation.

(L-L') and bottom surface (M-M'). The average equivalent plastic strain obtained along the top surface in the central steady state stable regime was approximately 1.09. The existence of low plastic strain regions at the work piece ends can be attributed to development of inclined (parallelogram) strain distribution pattern within the work piece.

Further, the rate at which the equivalent plastic strain increases at the top surface of the work piece with increasing number of ECAP passes through route #C was observed to be relatively high during odd passes (1^{st}, 3^{rd}) when compared to even passes. This can be attributed to the rotation of work piece by 180° after every pass which results in reversal of top and bottom surfaces, i.e., during the first pass, the top surface (AB in Fig. 7) of work piece was forced to pass through the sharp cornered inner channel angle resulting in high plastic strain. This top surface that had experienced a higher strain during the first pass gets transformed into bottom surface during the second pass (Fig. 7b). Now this surface 'AB' experiences lesser strain during this second pass. In the third pass, as the surfaces are reversed again, the surface 'AB' becomes the top surface and experiences a higher strain as it passes through the sharp inner channel angle. The rate of increase in equivalent plastic strain with increasing number of passes along bottom surface (M-M') was observed to be high during even passes (2^{nd}, 4^{th}) whereas a constant rate of increase in strain was observed along the middle region (L-L') with increasing number of ECAP pass through route #C.

The average equivalent plastic strain along the top, middle bottom surfaces was evaluated after each ECAP pass through route #C. It can be seen from Fig. 10 that after even pass, the average equivalent plastic strain along the top, middle and bottom surfaces is nearly equal. This indicates that a homogenous equivalent plastic strain distribution can be obtained in the material after every even numbered pass in ECAP through route #C. Further, the rate at which the average equivalent plastic strain increases with increasing number of passes through route #C along the middle region (L-L') was found to be linear. Whereas, the rate of increase in average equivalent plastic strain along the top and bottom surfaces were found to be nonlinear and quite different. Along the top surface, from first to second pass and from third to fourth pass, the rate of increase in the equivalent plastic strain (as evident from the slope of the line in Fig. 10) was found to be less while a higher rate of increase in strain was observed during the second to third ECAP pass. Whereas, the trend was found to be reverse along the bottom surface. These variations can be attributed to the rotation of the work piece by 180° during subsequent passes.

Excluding the highly inhomogeneous work piece ends ~ 20 mm on either side, the average equivalent plastic strain obtained from the analysis after each pass was compared with the values estimated using the analytical equation proposed by Iwahashi et al. [23]. It can be clearly seen from Fig. 11 that the average equivalent plastic strain obtained from FEA after excluding low strained work piece ends conform closely to that predicted by the analytical equation.

3.3. Load analysis

The load-displacement curves obtained from FEA during ECAP of pure aluminium through route #C are shown in Fig. 12. A three-stage pattern in the load-displacement curve was observed during the first ECAP pass: The load initially increases, attains a peak value (stage #1) and then decreases slightly to attain a constant value (stage #2) and remains constant throughout the pressing (stage #3). During the initial stages of deformation as the work piece enters

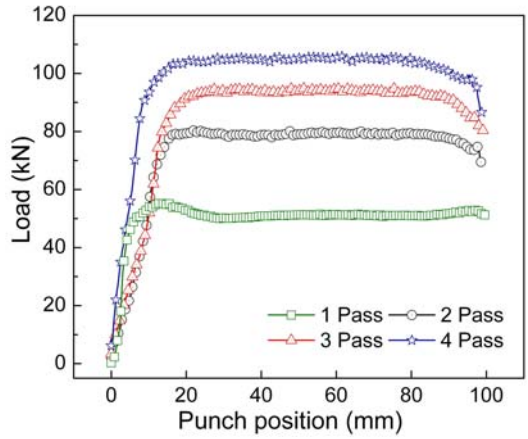

Fig. 12. Load-displacement curves during multiple ECAP.

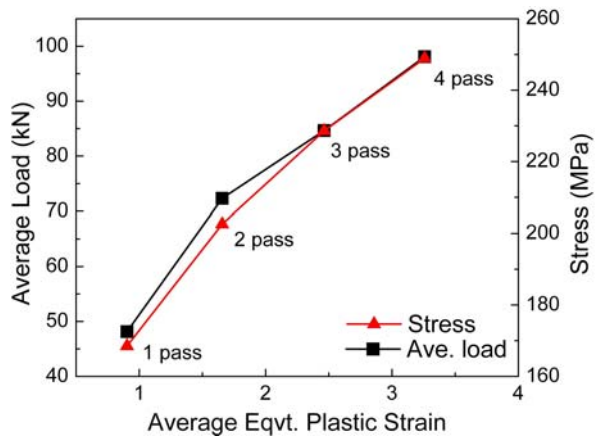

Fig. 13. Stress and average load required vs. average equivalent plastic strain after every pass.

the main deformation zone, it is obstructed by the outer channel surface. As the punch moves down, the work piece undergoes compression in the main deformation zone and hence the load increases. As the deformation progresses, sufficient amount of compression takes place and the work piece fills the main deformation zone and the load attains a peak value (stage #1). During further deformation, the work piece starts to slide on the outer channel surface, this sliding of the work piece along the outer channel surface causes shear deformation in the material and hence the load drops (stage #2). As the deformation progresses, the leading end of the work piece exits the main deformation zone and shear deformation takes place in other regions of the work piece, the load drops from the peak value and attains a steady state. Further deformation of the work piece then takes place under constant load (stage #3).

Such a three-stage load-displacement curve was not observed during the subsequent ECAP passes through route #C. This can be attributed to the change in the work piece shape or geometry after the first pass as shown in Fig. 6. However, the load required for pressing the work piece was found to increase with increasing number of ECAP passes. The rate of increase in load required to extrude the work piece decreases with increasing number of ECAP passes. This can be attributed to the constitutive material behaviour of pure aluminium. The same was confirmed by comparing the stress required to achieve an equivalent strain from the constitutive equation (Table 1) and the load obtained during ECAP through FEA. From Fig. 13 it can be clearly seen that the slope change observed in the load curve is similar to that observed in the stress curve.

4. Conclusions

Multi-pass ECAP simulation through route #C carried out in the present work with a round cornered die channel revealed the following:

– A stable and uniform plastic strain distribution in the material after every even pass.

– The rate of increase in strain along the length of the material at the top and bottom surfaces is influenced by the rotation of work piece after every pass, whereas the rate of increase in strain at mid surface is independent of work piece rotation.

– Front and back ends of the work piece exhibit very less strain as these regions experience very less deformation. The length of this less strained region is approximately equal to the ECAP channel width (w).

– Neglecting a length equivalent to the channel width (w) at both ends, a uniformly strained or deformed work piece can be obtained after every even numbered pass through route #C.

– The corner gap subtended by the work piece during subsequent ECAP passes through route #C was found to be independent of work piece geometry whereas the pattern of the load-displacement curve is influenced by the work piece shape or geometry.

Acknowledgements

The authors thank Dr. G. Malakondaiah, Director, Defence Metallurgical Research Laboratory (DMRL) for permitting us to publish this work. The authors acknowledge the funding provided by Defence Research and Development Organization (DRDO).

References

[1] SURYANARAYANA, C.: Int. Mater. Rev., *40*, 1995, p. 41.

[2] SEGAL, V. M.—REZNIKOV, V. I.—DROBYSHEVSKIY, A. E.—KOPYLOV, V. I.: Russ. Metall., *1*, 1981, p. 99.
[3] SAITO, Y.—TSUJI, N.—UTSUNOMIYA, H.—SAKAI, T.—HONG, R. G.: Scripta Mater., *39*, 1998, p. 1221. doi:10.1016/S1359-6462(98)00302-9
[4] SAITO, Y.—UTSUNOMIYA, H.—TSUJI, N.—SAKAI, T.: Acta Mater., *47*, 1999, p. 579. doi:10.1016/S1359-6454(98)00365-6
[5] VALIEV, R. Z.—KRASILNIKOV, N. A.—TSENEV, N. K.: Mat. Sci. Eng. A, *197*, 1991, p. 35. doi:10.1016/0921-5093(91)90316-F
[6] SALISHCHEV, G. A.—MIRONOV, S. YU.—ZHEREBTSOV, S. V.: Rev. Adv. Mater. Sci., *11*, 2006, p. 152.
[7] SEGAL, V. M.: Mat. Sci. Eng. A, 197, 1995, p. 157. doi:10.1016/0921-5093(95)09705-8
[8] DUMOULIN, S.—ROVEN, H. J.—WERENSKOID, J. C.—VALBERG, H. S.: Mat. Sci. Eng. A, *410–411*, 2005, p. 248. doi:10.1016/j.msea.2005.08.103
[9] SON H HEON—LEE JEONG HO—IM YONG TAEK: J. Mat. Process. Tech., *171*, 2006, p. 480. doi:10.1016/j.jmatprotec.2005.11.001
[10] BALASUNDAR, I.—SUDHAKARA RAO, M.—RAGHU, T.: Mat. Design, *30*, 2009, p. 1050. doi:10.1016/j.matdes.2008.06.057
[11] NAGASEKHAR, A. V.—TICK HON YIP—LI, S.—SEOW, H. P.: Mat. Sci. Eng. A, *410–411*, 2005, p. 269. doi:10.1016/j.msea.2005.08.043
[12] YOON, S. C.—KIM, H. S.: Mat. Sci. Eng. A, *490*, 2008, p. 438. doi:10.1016/j.msea.2008.01.066
[13] KIM, W. J.—NAMKUNG, J. C.: Mat. Sci. Eng. A, *412*, 2005, p. 287. doi:10.1016/j.msea.2005.08.222
[14] PRAGNELL, P. B.—HARRIS, C.—ROBERTS, S. M.: Scr. Mater., *37*, 1997, p. 983.
[15] SRINIVASAN, R.: Scr. Mater., *44*, 2001, p. 91. doi:10.1016/S1359-6462(00)00546-7
[16] SEMIATIN, S. L.—DELO, D. P.—SHELL, E. B.: Acta Mater., *48*, 2000, p. 1841. doi:10.1016/S1359-6454(00)00019-7
[17] SUH, J. Y.—KIM, H. S.—PARK, V.—CHANG, J. Y.: Scr. Mater., *44*, 2001, p. 677. doi:10.1016/S1359-6462(00)00645-X
[18] YANG, F. Q.—SARAN, A.—OKAZAKI, K.: J. Mater. Proc. Technology, *166*, 2005, p. 71. doi:10.1016/j.jmatprotec.2004.06.032
[19] KIM, H. S.: Mat. Sci. Eng. A, *328*, 2002, p. 317. doi:10.1016/S0921-5093(01)01793-2
[20] SHUBO XU—GUOQUN ZHAO—XINWU MA—GUOCHENG REN: J. Mater. Process. Technol., *184*, 2007, p. 209. doi:10.1016/j.jmatprotec.2006.11.025
[21] LEE, J. H.—SON, I. H.—IM, Y. T.—CHON, S. H.—PARK, J. K.: J. Mater. Process. Technol., *191*, 2007, p. 39. doi:10.1016/j.jmatprotec.2007.03.055
[22] ZHAO, W. J.—DING, H.—REN, Y. P.—HAO, S. M.—WANG, J.—WANG, J. T.: Mat. Sci. Eng. A, *410–411*, 2005, p. 348. doi:10.1016/j.msea.2005.08.134
[23] BOWEN, J. R.—GHOLINIA, A.—ROBERTS, S. M.—PRAGNELL, P. B.: Mat. Sci. Eng. A, *287*, 2000, p. 87. doi:10.1016/S0921-5093(00)00834-0
[24] CHENG XU—LANGDON, T. G.: Scr. Mater., *48*, 2003, p. 1. doi:10.1016/S1359-6462(02)00354-8
[25] SEMIATIN, S. L.—SEGAL, V. M.—GOFORTH, R. E.—FREY, N. D.—DELO, D. P.: Metall. Trans., *30A*, 1999, p. 1425.
[26] KIM, H. S.—SEO, M. H.—HONG, S. I.: Mat. Sci. Eng. A, *291*, 2000, p. 86. doi:10.1016/S0921-5093(00)00970-9
[27] IWAHASHI, Y.—WANG, J.—HORITA, Z.—NEMOTO, M.—LANGDON, T. G.: Scr. Mater., *35*, 1996, p. 143. doi:10.1016/1359-6462(96)00107-8
[28] SUO TAO—LI YULONG—GUO YAZHOU—LI YUANGYONG: Mat. Sci. Eng. A, *432*, 2006, p. 269. doi:10.1016/j.msea.2006.06.035